Critical role of parathyroid hormone (PTH) receptor-1 phosphorylation in regulating acute responses to PTH

Akira Maeda[a], Makoto Okazaki[a], David M. Baron[b], Thomas Dean[a], Ashok Khatri[a], Mathew Mahon[a], Hiroko Segawa[a], Abdul B. Abou-Samra[c], Harald Jüppner[a], Kenneth D. Bloch[b], John T. Potts, Jr.[a,1], and Thomas J. Gardella[a,1]

[a]Endocrine Unit, Massachusetts General Hospital and Harvard Medical School, Boston, MA 02114; [b]Anesthesia Center for Critical Care Research, Massachusetts General Hospital and Harvard Medical School, Boston, MA 02114; and [c]Hamad Medical Corporation, Doha, Qatar

Contributed by John T. Potts, Jr., January 31, 2013 (sent for review November 20, 2012)

Agonist-induced phosphorylation of the parathyroid hormone (PTH) receptor 1 (PTHR1) regulates receptor signaling in vitro, but the role of this phosphorylation in vivo is uncertain. We investigated this role by injecting "knock-in" mice expressing a phosphorylation-deficient (PD) PTHR1 with PTH ligands and assessing acute biologic responses. Following injection with PTH (1–34), or with a unique, long-acting PTH analog, PD mice, compared with WT mice, exhibited enhanced increases in cAMP levels in the blood, as well as enhanced cAMP production and gene expression responses in bone and kidney tissue. Surprisingly, however, the hallmark hypercalcemic and hypophosphatemic responses were markedly absent in the PD mice, such that paradoxical hypocalcemic and hyperphosphatemic responses were observed, quite strikingly with the long-acting PTH analog. Spot urine analyses revealed a marked defect in the capacity of the PD mice to excrete phosphate, as well as cAMP, into the urine in response to PTH injection. This defect in renal excretion was associated with a severe, PTH-induced impairment in glomerular filtration, as assessed by the rate of FITC-inulin clearance from the blood, which, in turn, was explainable by an overly exuberant systemic hypotensive response. The overall findings demonstrate the importance in vivo of PTH-induced phosphorylation of the PTHR1 in regulating acute ligand responses, and they serve to focus attention on mechanisms that underlie the acute calcemic response to PTH and factors, such as blood phosphate levels, that influence it.

calcium homeostasis | family B GPCR | phosphate homeostasis | receptor phosphorylation

Parathyroid hormone (PTH) plays a critical role in regulating blood concentrations of ionized calcium by acting via its receptor, the PTH receptor 1 (PTHR1), expressed by target cells of bone and kidney. In response to decreases in blood Ca^{2+} levels, PTH thus acts to promote the release of calcium from bone, and the reabsorption of calcium from the glomerular filtrate. PTH also acts to lower blood inorganic phosphate (Pi) by promoting the renal excretion of Pi into the urine. PTH acts in concert with several other calcium- and phosphate-regulating factors, including $1,25(OH)_2$-vitamin-D_3 and FGF23, as part of a tightly regulated homeostatic system of mineral ion control (1). Of note, PTH peptides injected daily at low dose can stimulate new bone formation and are thus in use to treat osteoporosis (2). Because of their calcemic actions, PTH peptides also hold promise as treatments for hypoparathyroidism (3).

The PTHR1 is a class B G protein-coupled receptor (GPCR) that signals via the Gαs/cAMP/PKA and Gαq/phopholipase C (PLC)/intracellular calcium (iCa)/PKC pathways (4). In cultured cells, agonist activation of the PTHR1 induces rapid receptor internalization and signal desensitization. As for most GPCRs, the PTHR1 is phosphorylated on its C-terminal tail following agonist activation, and this phosphorylation promotes the internalization and desensitization responses, in large part by stabilizing interaction with β-arrestins (5–9). Phosphorylation-deficient (PD) mutant PTH receptors that have key serine residues replaced by alanine are thus defective for mediating efficient β-arrestin recruitment, receptor internalization, and signal desensitization responses to PTH challenge (5–9). Genetically altered knock-in mice expressing such a PD-PTHR1 in place of the endogenous receptor exhibit prolonged blood cAMP elevations in response to injected PTH (1–34) and develop significant hypercalcemia after several days of continuous PTH (1–34) infusion (10). It is as yet unclear, however, whether or not PTHR1 phosphorylation plays a role in regulating the acute physiological actions of the PTHR1.

To explore further the functional importance of PTHR1 phosphorylation, we investigated whether or not acute biological responses to injected PTH ligands would be altered in the PD mice. We used for these studies unmodified PTH (1–34), as well as modified PTH analogs found to induce prolonged signaling actions in cells, as well as prolonged hypercalcemic and hypophosphatemic responses in animals (11, 12). The prolonged actions of these analogs correlate with their capacity to bind to a stable high-affinity PTHR1 conformation called R^0 (13, 14). Herein, we find that injection of either PTH (1–34) or the modified analogs into PD mice indeed results in enhanced elevations of cAMP in blood, bone, and renal tissue compared with in WT mice, but surprisingly the blood Ca and Pi responses were markedly blunted, as was the ligand-induced excretion of cAMP and Pi into the urine. The underlying mechanisms were revealed to involve effects on glomerular filtration, deriving, in turn, from enhanced effects on systemic blood pressure. Effects seen with PTH (1–34) were markedly exaggerated, and thus confirmed, with the modified peptides, most notably with the unique, very long-acting analog, LA-PTH.

Results

Properties of the PD-PTHR1 in Vitro. Comparison of the PD-PTHR1 to the WT-PTHR1 in cell-membrane–based binding assays designed to assess binding to two distinct high-affinity receptor conformations: a G protein-independent receptor conformation, R^0, and a G protein-dependent conformation, RG, as well as in cell-based assays of signaling via the cAMP/PKA, PLC/iCa/PKC, and ERK-1/2 pathways using unmodified PTH (1–34) as a probe, revealed only minor differences in the functional responses of the two receptors (Fig. 1 *A*–*D* and Fig. S1 *A* and *B*; Datasets S1, S2, S3, and S4). Of note, however, the cAMP assays revealed a higher basal, and proportionately higher PTH-induced signaling response for the PD-PTHR1 vs. the WT-PTHR1 (Fig. 1 *C* and *D*). Western blot analysis of cell membrane preparations (Fig. S1*C*), indicated that the PD-PTHR1 was expressed at lower levels than the WT-PTHR1; thus, the higher basal cAMP signaling levels of the PD-PTHR1 likely arose from a higher level of ligand-independent signaling activity. Assessment

Author contributions: A.M., M.O., D.M.B., H.J., K.D.B., J.T.P., and T.J.G. designed research; A.M., M.O., D.M.B., T.D., and H.S. performed research; A.K., M.M., and A.B.A.-S. contributed new reagents/analytic tools; A.M., M.O., D.M.B., H.J., K.D.B., J.T.P., and T.J.G. analyzed data; and A.M., J.T.P., and T.J.G. wrote the paper.

The authors declare no conflict of interest.

[1]To whom correspondence may be addressed. E-mail: gardella@helix.mgh.harvard.edu or potts.john@mgh.harvard.edu.

This article contains supporting information online at www.pnas.org/lookup/suppl/doi:10.1073/pnas.1301674110/-/DCSupplemental.

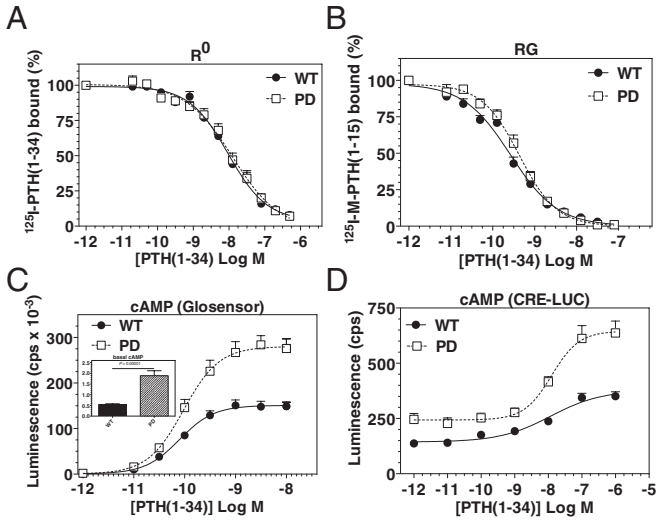

Fig. 1. Functional properties of the PD-PTHR1 in vitro. (*A*) Binding of PTH (1–34) to the WT-PTHR1 and PD-PTHR1 in the G protein-independent conformation, R^0. (*B*) Binding of PTH (1–34) to the WT- and PD-PTHR1 in the G protein-dependent conformation, RG. Binding was assessed by competition methods in COS-7 cell membranes. (*C*) cAMP signaling in response to PTH (1–34) by HEK-293 cells stably transfected to express either the WT-PTHR1 or PD-PTHR1 along with a luciferase-based glosensor cAMP reporter. (*Inset*) Basal luciferase activity in cells treated with buffer alone. (*D*) cAMP signaling assessed in HEK-293 cells transiently transfected to express either the WT-PTHR1 or PD-PTHR1 along with a CRE-Luc reporter. Data are means (±SEM) of six (*A* and *B*), or four (*C* and *D*) experiments, each in duplicate. Binding and signaling parameters are reported in Datasets S1, S2, S3, and S4.

of ligand-induced receptor internalization using a fluorescently labeled PTH(1–34)^{TMR} (where TMR is tetramethylrhodamine) analog and confocal microscopy revealed in cells expressing the WT-PTHR1 the formation of numerous fluorescent punctae that were dispersed within the cytoplasm at 5 min after ligand addition, and then became more perinuclear by 30 min (Fig. S1*D*). In cells expressing the PD-PTHR1, the fluorescence was initially weak and diffuse at 5 min, and then some punctae were apparent at dispersed locations by 30 min. The overall results of these in vitro studies are largely consistent with prior studies (5–7, 15), and thus show that the PD-PTHR1 is at least as functional as the WT-PTHR1 in terms of its capacity to bind PTH ligands and activate second-messenger signaling pathways, and exhibits at least some delay in ligand-induced internalization responses.

Effects of PTH (1–34) on Ca^{2+} and Pi Levels in Blood and Urine of WT- and PD Mice. Before injection, the concentration of Ca^{2+} in the blood of PD mice was not different from that of WT mice (~1.25 mM, Fig. 2*A*). Following injection of PTH (1–34) into WT mice, blood Ca^{2+} levels increased to ~1.35 mM at 1 to 2 h postinjection, and then returned to vehicle-control levels by 4 h; in contrast, blood Ca^{2+} in PD mice did not rise following PTH (1–34) injection but rather declined moderately at 1 h postinjection and then returned to vehicle levels by 2 h (Fig. 2*A*). PTH (1–34) injection into WT mice lowered blood Pi levels at 1 to 2 h postinjection; in contrast, blood Pi levels did not decrease in PD mice following PTH (1–34) injection, but remained at or near vehicle-control levels for at least 4 h (Fig. 2*B*). Thus, both the acute calcemic and hypophosphatemic responses to PTH (1–34) injection were blunted in PD mice. At later times (4–8 h) after PTH injection, blood Pi levels in both WT and PD mice tended to increase above vehicle levels. Whereas the early phase hypophosphatemic response to PTH (1–34), observed here only in WT mice, can be attributed to the rapid, PTH-induced down-regulation of the Pi transporter, NPT2a, in renal proximal tubule cells (16), the later-phase hyperphosphatemic response likely involves the PTH-induced increase in bone resorption.

Little or no change was detected in the concentration of calcium in the urine collected from either WT or PD mice at times after injection of PTH (1–34) (Fig. 2*C*). Urine Pi levels increased strongly at 1 and 2 h following injection of PTH (1–34) in WT mice, but no increase was observed in PD mice (Fig. 2*D*).

Analysis of the PD-PTHR1 with Modified PTH Analogs. To assess further the functional properties of the PD-PTHR1, we used the N-terminally modified PTH analog M-PTH (1–34) (11), and a long-acting M-PTH/PTHrP hybrid analog called LA-PTH. Compared with PTH (1–34), these two analogs bound with severalfold higher affinity to the R^0 conformation of both the WT-PTHR1 and PD-PTHR1 (Fig. S2; Dataset S1), mediated more prolonged cAMP responses following ligand wash-out in cells expressing either the WT or PD receptor (Fig. S3 *A–F*; Dataset S5), exhibited at least similar capacities to activate iCa signaling via either receptor (Fig. S3 *G* and *H*; Dataset S4), and, in WT mice, mediated more prolonged increases in urinary cAMP and blood Ca^{2+} (Fig. S4).

Calcemic and Phosphaturic Actions of PTH Analogs in WT and PD Mice. In WT mice, injection of LA-PTH induced a robust increase in blood Ca^{2+} that lasted for at least 8 h; in contrast, injection of the analog into PD mice caused blood Ca^{2+} levels to decline to below vehicle-control levels, and this reduction lasted for at least 6 h (Fig. 3*A*). In WT mice, LA-PTH injection caused reductions in blood Pi levels that persisted for at least 6 h; in contrast, blood Pi levels in PD mice injected with LA-PTH never decreased, but rather remained within vehicle-control levels for the initial 2 h and then rose to above vehicle-control levels at 4 and 6 h before returning to vehicle levels by 8 h (Fig. 3*B*). Similar paradoxical effects on blood Ca^{2+} and Pi were observed in the PD mice following injection with M-PTH (1–34) (Fig. S5 *A* and *B*). Little or no change was detected in the concentration of urine calcium in either WT or PD mice after injection of LA-PTH (Fig. 3*C*). Urine Pi levels in WT mice rose rapidly after injection of LA-PTH, with the peak increase occurring by 1 h after injection, and returned

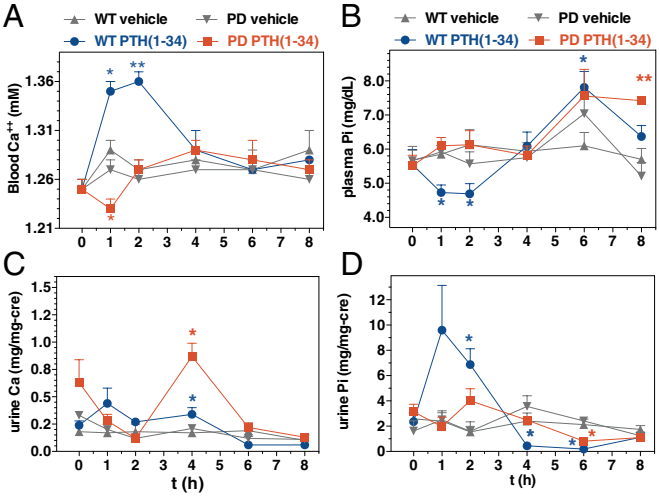

Fig. 2. Effects of PTH (1–34) on Ca^{2+} and Pi levels in blood and urine of WT and PD mice. (*A*) Mice were injected s.c. with either vehicle or PTH (1–34) (50 nmol/kg); tail vein blood was collected immediately before injection ($t = 0$) and at times thereafter and assessed for ionized calcium. (*B*) Mice were injected as in *A* and blood plasma was assessed for the concentration of inorganic phosphate (Pi). (*C*) Spot urine collected from the mice used in the experiment of *B* was assessed for total Ca. (*D*) Spot urine collected as in *C* was assessed for Pi. Data are means ± SEM; $n = 5$ mice per group (urine data are from three to five samples per time point); *P* vs. corresponding vehicle: $*P \leq 0.05$, $**P \leq 0.01$, $***P \leq 0.001$.

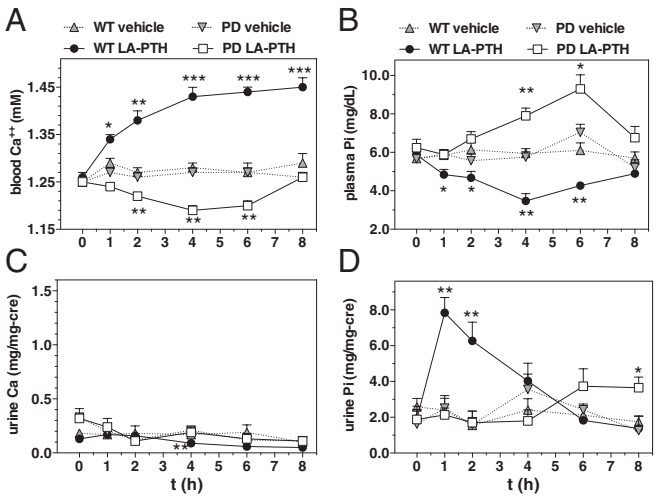

Fig. 3. Effects of a long-acting analog, LA-PTH, on Ca^{2+} and Pi levels in blood and urine of WT and PD mice. (*A*) Mice were injected s.c. with vehicle or LA-PTH (10 nmol/kg) and tail vein blood was collected and assessed for the concentration of Ca^{2+}. Note that in separate experiments, blood Ca^{2+} levels in both WT and PD mice injected with LA-PTH returned to vehicle-control levels by 48 h after injection. (*B*) Mice were injected as in *A*, and blood plasma was assessed for the concentration of Pi. (*C*) Spot urine collected from the mice used in the experiment of *B* was assessed for total Ca. (*D*) Spot urine collected as in *C* was assessed for Pi. Data are means ± SEM; $n = 5$ mice per group (urine data are from 3 to 5 samples per time point); *P* vs. corresponding vehicle: $^{*}P \leq 0.05$, $^{**}P \leq 0.01$, $^{***}P \leq 0.001$.

to baseline by 4 h. In contrast, urine Pi levels in PD mice did not change for the first 4 h after LA-PTH injection, and then increased modestly at 6 to 8 h (Fig. 3*D*).

Effects of PTH Analogs on cAMP Levels in Blood and Urine of WT and PD Mice. Injection of PTH (1–34) induced rapid increases in blood cAMP levels in both WT and PD mice, and the maximum increase in the PD mice was significantly greater than that in WT mice (10-fold vs. sixfold at 30 min postinjection, relative to initial; Fig. 4*A*). Urine cAMP levels in WT mice increased ~20-fold by 15 min after injection of PTH (1–34), whereas in striking contrast the urine cAMP levels in PD mice did not change following PTH (1–34) injection (Fig. 4*B*). Similarly, whereas injection of LA-PTH resulted in rapid and robust increases in cAMP in both blood and urine of WT mice, the analog increased cAMP levels in the blood, but not urine of PD mice (Fig. 4 *C* and *D*).

Effects of PTH Analogs on Signaling in Bone and Kidney of WT and PD Mice. To assess PTHR1 signaling directly in target tissues, we measured the levels of cAMP in homogenized kidneys and calvaria isolated from mice 15 min after PTH injection. Injection of PTH (1–34) resulted in two- to sixfold increases (vs. vehicle) in cAMP levels in both kidney and bone tissues of WT mice, and similar, if not enhanced, increases in cAMP were observed in the kidney and bone tissues of PD mice (Fig. 5 *A* and *B*). Injection of LA-PTH also increased cAMP levels in both target tissues of both mice, and the increases were again greater ($P < 0.05$) in PD mice than in WT mice (Fig. 5 *C* and *D*).

We then evaluated the effects of PTH (1–34) injection on the levels of expression of several known PTH-response genes in bone and kidney tissue. Injection of PTH (1–34) into WT mice resulted in a 2.5-fold increase in the levels of mRNA for RANK-ligand, a PTH-responsive osteoblast factor involved in osteoclast activation in calvarial bone, and a significantly greater, 13-fold increase in RANK-L mRNA was observed in PD mice (Fig. 6*A*). The mRNA for osteoprotegerin (OPG), an osteoblast factor which inhibits RANK-L and is down-regulated by PTH, was reduced fivefold in calvaria of both WT and PD mice following PTH (1–34) injection (Fig. 6*B*). Consistent with a greater effect on RANK-L expression in PD mice than in WT mice, blood levels of type I collagen C-telopeptide (CTX), a marker of bone resorption, were elevated in PD mice 1.5-fold at 3 h after PTH (1–34) injection (*P* vs. vehicle = 0.002), whereas no increase in CTX was detected in WT mice (Fig. S6*A*).

In the kidneys of both WT and PD mice, PTH (1–34) injection resulted in five- to sevenfold increases in the levels of mRNA for CYP27B1, which encodes the 1αhydroxylase that mediates PTH-induced synthesis of active $1,25(OH)_2$-vitamin-D_3 in the proximal tubule, and two- to threefold decreases in the levels of mRNA for CYP24A1, which encodes the 1,25-dihydroxyvitamin-D_3 24-hydroxylase that mediates the renal metabolism of 1,25-dihydroxyvitamin-D_3 (Fig. 6 *C* and *D*). Overall, these findings establish that upstream cAMP signaling, as well as certain hallmark downstream gene expression responses to PTH injection in bone and kidney tissues, is largely intact, if not enhanced, in the PD mice. The defects in certain downstream physiologic responses to PTH injection observed in the PD mice—i.e., the failure to export cAMP and Pi into the urine—are thus not likely due to impaired upstream signaling responses in these target tissues.

Effects of PTH (1–34) on Renal Filtration and Systemic Blood Pressure in WT and PD Mice. The failure of the PD mice to excrete Pi and cAMP into the urine in response to PTH injection, despite normal or even enhanced cAMP responses in the kidney, suggested that PTH injection into the PD mice might cause impairment in renal filtration/clearance. Related to this, we found that whereas blood levels of $1,25(OH)_2$-vitamin-D_3 in WT mice were elevated 6 h after PTH (1–34) injection by 2.5-fold (*P* vs.

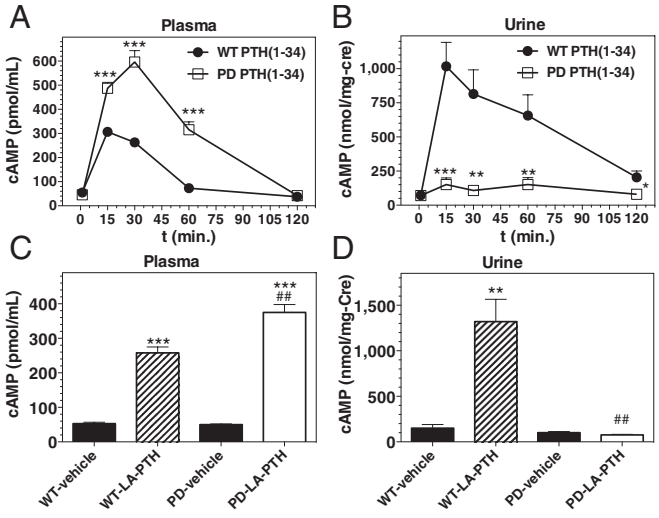

Fig. 4. Effects of PTH analog injection on cAMP levels in blood and urine of WT and PD mice. (*A*) Mice were injected s.c. with PTH (1–34) (50 nmol/kg); tail vein blood was collected immediately before injection ($t = 0$) and at times thereafter and the plasma was analyzed for cAMP. (*B*) Spot urine collected from the mice used in the experiment of *A* was analyzed for cAMP and creatinine (Cre). (*C*) Mice were injected with vehicle or LA-PTH (10 nmol/kg) and tail vein blood was collected at 15 min after injection; the plasma was analyzed for cAMP. (*D*) Spot urine from the mice used in the experiment of *C* was collected at 15 min after injection and analyzed for cAMP and creatinine (Cre). Note that in a separate, longer-term, experiment, no increase in urinary cAMP was detected in the PD mice at 3 and 6 h after injection of LA-PTH. Data are means ± SEM; $n = 8$ (*A* and *B*), or 5 (*C* and *D*) mice per group; urine data in *B* are from 5 to 8 samples for each time point; *P* vs. corresponding vehicle: $^{*}P \leq 0.05$, $^{**}P \leq 0.01$, $^{***}P \leq 0.001$; *P* vs. corresponding WT: $^{\#}P \leq 0.05$, $^{\#\#}P \leq 0.01$, $^{\#\#\#}P \leq 0.001$.

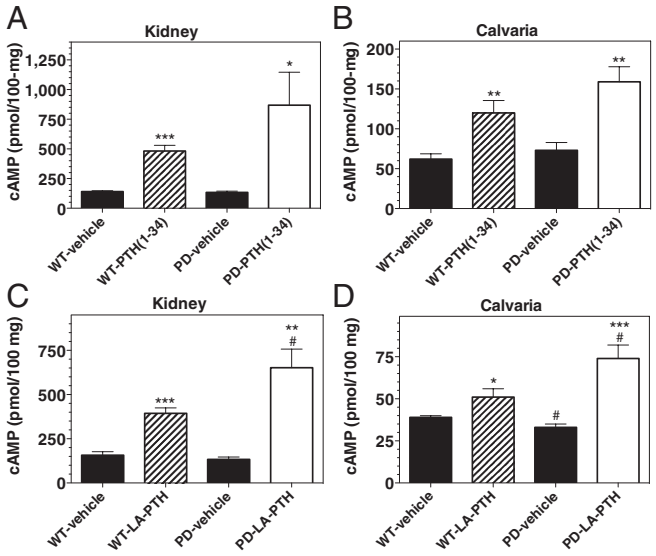

Fig. 5. Effects of PTH analog injection on cAMP levels in bone and kidney of WT and PD mice. (*A*) Mice were injected s.c. with vehicle or PTH (1–34) (50 nmol/kg) and 15 min after injection kidneys were isolated, homogenized, and the homogenates were analyzed for cAMP. (*B*) Homogenized calvaria isolated from the mice used in the experiment of *A* were analyzed for cAMP. (*C*) Mice were injected s.c. with LA-PTH (10 nmol/kg) and 15 min after injection kidneys were isolated, homogenized, and the homogenates were analyzed for cAMP. (*D*) Homogenized calvaria from the mice used in the experiment of *C* were analyzed for cAMP. Values of cAMP are expressed relative to 100 mg of tissue; data are means ± SEM; $n = 5$ mice per group; *P* vs. corresponding vehicle: $^{*}P \le 0.05$, $^{**}P \le 0.01$, $^{***}P \le 0.001$; *P* vs. corresponding WT: $^{\#}P \le 0.05$, $^{\#\#}P \le 0.01$, $^{\#\#\#}P \le 0.001$.

vehicle = 0.008), there was no increase in blood 1,25$(OH)_2$-vitamin-D_3 levels in PD mice (Fig. S6*B*), despite the changes in the renal hydroxylase mRNAs (Fig. 6 *C* and *D*). As renal production of 1,25$(OH)_2$-vitamin-D_3 is dependent on the uptake of the precursor, 25-hydroxyvitamin-D, from the urine, the failure of blood 1,25$(OH)_2$-vitamin-D_3 levels to increase upon PTH injection in PD mice could also be explained by impaired renal filtration, and hence reduced precursor availability. To assess effects on renal filtration, we injected WT and PD mice with FITC-labeled inulin, either alone or together with PTH (1–34), and then measured the rate of FITC-inulin clearance from the blood (17). Coinjection of PTH (1–34) caused little or no change in the rate of clearance of the marker in WT mice, but it markedly diminished the rate of clearance in PD mice (Fig. 7*A*). Without PTH coinjection, the blood clearance rates of FITC-inulin were similar in WT and PD mice. Estimations of glomerular filtration rate (GFR) from these data indicated that whereas PTH (1–34) injection did not significantly alter GFR in WT mice [215 ± 15 vs. 176 ± 24 μL/min; vehicle vs. PTH (1–34); $P > 0.05$], it reduced GFR in PD mice by at least 10-fold (248 ± 31 vs. 21 ± 3 μL/min; $P = 0.0003$). An even more prolonged reduction in FITC-inulin clearance was observed in PD mice upon coinjection of LA-PTH (Fig. 7*B*).

As PTH is known to have hypotensive effects on the vasculature (18), and previous studies in rats show that PTH-induced reductions in systemic blood pressure can result in reduced glomerular blood flow (19), we assessed the effects of PTH administration on systemic blood pressure in WT and PD mice (20). Following a brief i.v. infusion of PTH (1–34) (50 nmol/kg over 2 min of infusion), left ventricular (LV) end-systolic pressure (ESP) declined rapidly in both WT and PD mice, but the decline was significantly greater in PD mice than in WT mice (Fig. 7*C*). Injection of PTH (1–34) into PD mice did not reduce cardiac output or LV end-diastolic pressure (Fig. S7 *A* and *B*), consistent with vasodilation mediating the effects of PTH on blood pressure.

Discussion

It is evident from these studies that physiological responses to injected PTH ligands are acutely and severely perturbed in mice bearing the PD PTHR1 knock-in mutation, compared with responses in WT mice. The altered responses observed in the PD mice with PTH (1–34) were confirmed and indeed exaggerated with the longer-acting analogs, M-PTH (1–34) and LA-PTH. Whereas responses in bone appeared, if anything, enhanced in the PD mice, as shown by the more pronounced increases in calvarial cAMP and RANK-L mRNA, certain renal responses, namely the PTH-induced export of cAMP into the urine, and the phosphaturic response, were markedly defective. These defects in renal function were not associated with defects in either upstream PTH signaling or immediate downstream responses in the kidneys of the PD mice, as shown by the robust inductions in the levels of cAMP and CYP27B1 mRNA in kidney tissue isolated from the mice after injection. The defects in blood and urine responses observed in the PD mice were, however, associated with marked PTH-induced reductions in renal filtration, as revealed by the severely reduced rates of FITC-inulin clearance.

The PD mice further exhibited an overly exuberant systemic hypotensive response to PTH injection, which could well account for the defects in renal filtration (19). This enhancement in the PTH-induced hypotensive response presumably reflects a defect in the capacity of the PD-PTHR1 to desensitize and/or down-regulate in vasculature cells following PTH activation. The PTHR1 is known to be expressed in vascular smooth muscle and endothelial cells and to mediate reductions in vascular tone (18). A defect in desensitization is also likely reflected by the higher basal and PTH-induced cAMP signaling responses observed for the PD-PTHR1 in our in vitro assays, and likely contributes to the normalization of the blood Ca^{2+} and Pi levels observed in the

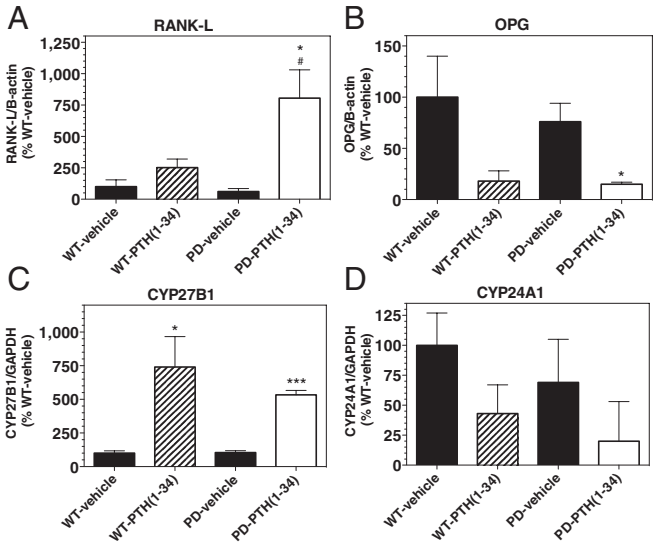

Fig. 6. Effects of PTH analog injection on PTH target gene mRNA levels in bone and kidney of WT and PD mice. (*A*) Mice were injected s.c. with vehicle or PTH (1–34) (50 nmol/kg) and 2 h after injection calvarial bones were isolated, homogenized, and the homogenates were analyzed by RT-PCR for mRNA encoding RANK-L. (*B*) Calvarial homogenates used in *A* were also assessed for mRNA encoding OPG. (*C*) Kidneys isolated from the mice used in the experiment of *A* and *B* were analyzed for mRNA encoding CYP27B1, the 25-hydroxyvitamin-D_3-1,α-hydroxylase. (*D*) Kidney homogenates were also analyzed for mRNA encoding CYP24A1, the 1,25-dihydroxyvitamin-D_3 24-hydroxylase. Data are means ± SEM; $n = 4$–5 mice per group; *P* vs. corresponding vehicle: $^{*}P \le 0.05$, $^{**}P \le 0.01$; $^{***}P \le 0.001$; *P* vs. corresponding WT: $^{\#}P \le 0.05$, $^{\#\#}P \le 0.01$, $^{\#\#\#}P \le 0.001$.

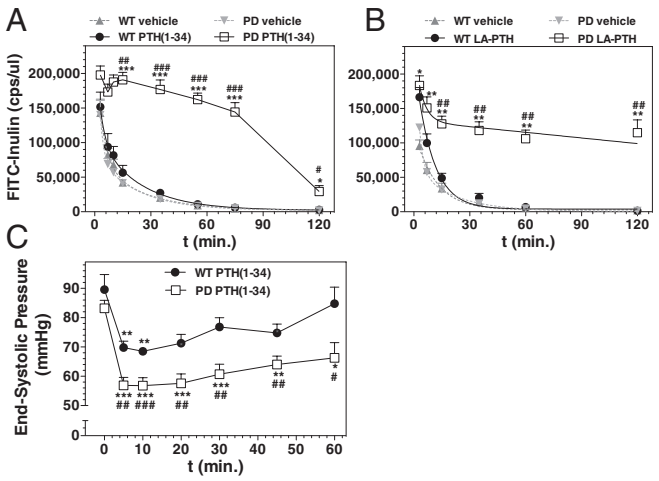

Fig. 7. Effects of PTH analog injection on renal filtration and systemic blood pressure in WT and PD mice. (*A*) Mice were injected via the tail vein with FITC-inulin alone (vehicle) or FITC-inulin with PTH (1–34) (50 nmol/kg), and tail vein blood was collected at times thereafter; the plasma was assessed for FITC fluorescence. (*B*) Mice were injected with FITC-inulin alone (vehicle) or FITC-inulin with LA-PTH (10 nmol/kg), and blood was analyzed as in *A*. (*C*) Anesthetized mice were infused i.v. with PTH (25 nmol·kg^{-1}·min^{-1}) for 2 min, and ESP was measured at the LV (t = 0 indicates immediately before PTH infusion). Data are means ± SEM; n = 3 (*A*, vehicle and *B*), 4 [*A*, PTH (1–34)-injected], or 6 (*C*) mice per group; P vs. corresponding initial: $^{*}P \le 0.05$, $^{**}P \le 0.01$; $^{***}P \le 0.001$; P vs. corresponding WT: $^{\#}P \le 0.05$, $^{\#\#}P \le 0.01$, $^{\#\#\#}P \le 0.001$.

PD mice in the context of their lower endogenous levels of PTH (1–84), as found previously (21).

We also observed that whereas injection of PTH (1–34) into WT mice induced the expected reduction in NPT2a protein levels in renal brush border membranes, it failed to do so in PD mice (Fig. S8 *A–D*). This finding could conceivably indicate a defect in some PTHR function, as yet unknown but likely other than cAMP signaling per se, in renal proximal tubule cells that is involved in the PTH-induced down-regulation of NPT2a (16, 22). It seems at least equally likely, however, given the current findings, that the results reflect a reduced access of the ligand to renal receptors, especially on the luminal membrane surface (23), due to impaired filtration. The fact that the injected PTH ligands increased cAMP in kidney tissue of the PD mice to at least the same extent as they did in WT mice, and also increased CYP27B1 mRNA, confirms that the ligands gained access to at least the blood or basolateral surface of renal target cells. The mechanisms by which PTH induces the export of cAMP into the urine by renal cells is not known, but the lack of a urinary cAMP response in the PD mice, coupled with the increased cAMP levels in the blood and renal tissues, together with the markedly reduced GFR, further supports a model by which the injected PTH had reduced access to the apical surfaces of renal tubules.

Perhaps the most surprising finding in these studies was the hypocalcemic response to PTH (1–34) and long-acting analogs. This hypocalcemia occurred despite the findings that the increases in cAMP, as well as RANK L mRNA, in bone, and increases in CTX in blood, were greater in the PD mice than in the WT mice, confirming that the bone response to PTH was, if anything, enhanced in the PD mice. A more exuberant bone response to PTH in the PD mice is further suggested by the finding that the blood Pi levels rose to significantly above vehicle levels by 4 h following injection with LA-PTH (Fig. 3*B*), as this elevation in blood Pi most likely arises from a robust bone-resorption response, coupled with a defect in Pi excretion. As discussed below, it seems plausible that the failure of blood Ca levels to rise in PD mice following PTH injection is related to the failure of blood Pi levels to fall, which, in turn, is related to the impairment in GFR. In the prior study of Bounoutas et al., a frank hypercalcemic response was indeed observed in PD mice following 3 d of PTH (1–34) infusion (10). This hypercalcemic response can likely be accounted for by the lower dose and slower route of PTH administration (7 nmol/kg over a 24-h infusion) used in that study, which was likely too low to induce the marked reductions in blood pressure, GFR, and hence Pi clearance, as were observed in our studies, in which PTH was administered at higher doses (10–50 nmol/kg) and as single bolus injections.

The fact that hypocalcemia occurred in our study at 4 h after LA-PTH injection, when blood Pi levels were significantly above normal, may not be unexpected given the known capacity of blood Pi infusion to lower blood Ca (24, 25). It is the earlier fall in blood Ca in the PD mice observed at 1 to 2 h after PTH injection, when blood Pi levels were near normal, that seems particularly surprising. Earlier reports, however, highlight the importance of the rapid phosphaturic action of PTH and the associated lowering of blood Pi for the hypercalcemic response (25–27). Thus, Parsons et al. showed in dogs and rats that PTH injection first induces a hypocalcemic effect that occurs before the fall in blood Pi, after which blood Ca increases (28, 29). Raisz et al. showed in vitro a damping effect of Pi on the PTH-induced release of Ca from bone calvaria (30).

The PTH-induced hypocalcemic effect noted by Parsons was demonstrated by radio-calcium labeling methods to be due to a transient flux of Ca from blood into bone (29). Our studies do not provide direct evidence for such a mechanism, but they nevertheless serve to focus attention on the nature of the rapid response in calcium transport systems stimulated by PTH. A working hypothesis is that these transport systems are affected by ambient Pi concentrations, and that the absence of a fall in blood Pi in the PD animals, resulting from the hypotension-induced block in GFR, accounts for the early hypocalcemia. Because these systems must be an important element of the overall homeostatic regulation of calcium by PTH, efforts to further characterize them and the cell types involved are important topics for further study.

Materials and Methods

Peptides. Human PTH analogs used were PTH (1–34), M-PTH (1–34) (M= Ala^{1,12},Aib^{3},Gln^{10},Har^{11},Trp^{14},Arg^{19}); and M-PTH (1–15), the latter containing the M modifications as well as Nle^{8} and Tyr^{15}. LA-PTH contained the hPTH (1–14) sequence modified with Ala^{1,3,12},Gln^{10},Arg^{11},Trp^{14}, followed by the hPTHrP (15–36) sequence modified with Ala^{18,22} and Lys^{26} (31). Radioligands used were ^{125}I-PTH (1–34) ([^{125}I-[Nle^{8,21},Tyr^{34}]ratPTH(1–34)NH$_2$) and ^{125}I-M-PTH (1–15) (^{125}I-[Aib^{1,3},Nle^{8},Gln^{10},Har^{11},Ala^{12},Trp^{14},Tyr^{15}]PTH(1-15)NH$_2$) (14). (TMR)-PTH (1–34) contained TMR attached to the epsilon amino group of Lys^{13}. Peptides contained C-terminal amides, except LA-PTH and PTH (1–34), which contained free C-terminal carboxyl groups.

PTHR1 Binding, Signaling, and Microscopy. Binding to the RG and R^{0} conformations of the rat PTHR (WT or PD) was assessed by competition methods using COS-7 cell membranes, as described in ref. 14. Binding to R^{0} was assessed using ^{125}I-PTH (1–34) tracer radioligand, and GTPγS (1×10^{-5} M) was added to the reactions. Binding to RG was assessed using membranes containing a high-affinity Gα$_s$ mutant (Gα$_s^{ND}$) and ^{125}I-M-PTH (1–15) tracer radioligand. Signaling via the cAMP/PKA pathway was assessed using HEK-293-derived cell lines that stably express the Glosensor cAMP reporter (Promega Corp.) (32), along with either the WT rat PTHR1 (GR-35 cells) or the PD rat PTHR1 (GPD-4 cells). cAMP responses were also assessed using HEK-293 cells transiently transfected to express a cAMP-response-element/luciferase (Cre-Luc) reporter (33), and either the WT or PD rat PTHR1. Intracellular calcium (iCa^{++}) signaling was assessed in transiently PTHR1-transfected HEK-293 cells using Fura2-AM (Invitrogen, Life Tech.) (22). cAMP and iCa^{++} signaling assays were performed in 96-well plates and analyzed using a PerkinElmer Envision plate reader. Signaling via the ERK1/2 pathway was assessed by Western blot using antibodies (Cell Signaling Tech. Inc.) specific for phospho- or total ERK1/2. Confocal microscopy was performed using cells fixed and mounted at times after TMR-PTH (1–34) (100 nM) addition, and a Bio-Rad/Zeiss Radiance 2000 confocal microscope (Carl Zeiss MicroImaging Inc.).

Physiologic Responses in Mice. Mice (male C57BL/6, aged 8–19 wk) were treated following the ethical guidelines adopted by the Massachusetts General Hospital. WT mice were obtained from Charles River Laboratory.

Homozygous PD knock-in mice (10) were maintained at the MGH. Mice were injected s.c. with vehicle (10 mM citric acid/150 mM NaCl/0.05% Tween-80, pH 5.0) or vehicle containing PTH (1–34) or M-PTH (1–34) at doses of 50 nmol/kg or LA-PTH at 10 nmol/kg. Blood was collected from the tail vein and analyzed directly for Ca^{2+} using a Siemens RapidLab 348 Ca^{2+}/pH analyzer; or as plasma for Pi using a photometric assay (Wako Laboratory); cAMP in plasma, urine, and tissue homogenates was measured by RIA; plasma levels of 1,25$(OH)_2$-vitamin-D_3 and CTX were measured using EIA kits (IDS Ltd.). Urine creatinine was measured using a photometric assay (Stanbio Laboratory).

Tissue mRNA. Mouse kidneys and calvaria were harvested, frozen in liquid nitrogen, homogenized in TRIzol (Invitrogen), and mRNA was purified using the RNeasy Plus mini kit (Qiagen), quantified using a NanoDrop 8000 UV spectrophotometer (Thermo Scientific), and processed using a QuantiTect Reverse Transcription kit (QIAGEN catalog no. 205313), a QuantiFastSYBER Green PCR kit (Qiagen catalog no. 204054), and a StepOnePlus PCR instrument (Applied Biosystems). PCR primers are shown in Fig. S9**).**

FITC-Inulin Clearance and Blood Pressure Measurements. FITC-inulin [Sigma; dialyzed (molecular weight cutoff = 1,000] vs. 150 mM NaCl, was injected via the tail vein, either alone (vehicle) or together with either PTH (1–34) (50 nmol/kg) or LA-PTH (10 nmol/kg). Tail vein blood was then collected and the plasma was assessed for FITC fluorescence (λ excitation = 480 nm; λ emission = 530 nm) using a PerkinElmer-Victor3 plate reader. GFR was calculated by fitting the data to a biexponential decay function and using the equation GFR = $I/(A/\alpha) \pm B/\beta)$, where I is ligand dose, A and B are the *y* intercepts of the two decay components, and α and β are the corresponding decay constants (17). Cardiac blood pressure was measured as described in ref. 20; mice were anesthetized by i.p. injection with ketamine (100 mg/kg), fentanyl (50 mg/kg), and rocuronium (2 mg/kg), intubated, and mechanically ventilated (fraction of inspired O_2 =1, 10 mL/g, 120 breaths per minute). The chest was opened, and a pressure–volume conductance catheter (PVR-1030; Millar Instruments) was introduced through the apex into the left ventricle and used to measure ESP. A second catheter inserted into the right jugular vein was used to administer PTH (1–34) (25 $nmol \cdot kg^{-1} \cdot min^{-1}$) via a perfusor pump at a rate of 1.25 $\mu L \cdot g^{-1} \cdot min^{-1}$ for 2 min.

Data Calculations. Data were processed using Excel 2008 (Microsoft Corp.) and Prism 5.0 (GraphPad Software Inc.). Statistical analyses used the Student *t* test (two-tailed, unequal variances), with significance inferred from *P* values of 0.05 or less.

ACKNOWLEDGMENTS. Monica Reyes assisted with animal breeding. This work was supported by National Institutes of Health Grant DK-11794.

1. Bergwitz C, Jüppner H (2010) Regulation of phosphate homeostasis by PTH, vitamin D, and FGF23. *Annu Rev Med* 61:91–104.
2. Neer RM, et al. (2001) Effect of parathyroid hormone (1-34) on fractures and bone mineral density in postmenopausal women with osteoporosis. *N Engl J Med* 344(19): 1434–1441.
3. Winer KK, et al. (2012) Synthetic human parathyroid hormone 1-34 replacement therapy: A randomized crossover trial comparing pump versus injections in the treatment of chronic hypoparathyroidism. *J Clin Endocrinol Metab* 97(2):391–399.
4. Vilardaga JP, Romero G, Friedman PA, Gardella TJ (2011) Molecular basis of parathyroid hormone receptor signaling and trafficking: A family B GPCR paradigm. *Cell Mol Life Sci* 68(1):1–13.
5. Tawfeek HA, Qian F, Abou-Samra AB (2002) Phosphorylation of the receptor for PTH and PTHrP is required for internalization and regulates receptor signaling. *Mol Endocrinol* 16(1):1–13.
6. Vilardaga J, et al. (2002) Internalization determinants of the parathyroid hormone receptor differentially regulate beta arrestin/receptor association. *J Biol Chem* 277(10):8121–8129.
7. Chauvin S, Bencsik M, Bambino T, Nissenson RA (2002) Parathyroid hormone receptor recycling: Role of receptor dephosphorylation and beta-arrestin. *Mol Endocrinol* 16(12):2720–2732.
8. Rey A, Manen D, Rizzoli R, Ferrari SL, Caverzasio J (2007) Evidences for a role of p38 MAP kinase in the stimulation of alkaline phosphatase and matrix mineralization induced by parathyroid hormone in osteoblastic cells. *Bone* 41(1):59–67.
9. Wang B, Yang Y, Abou-Samra AB, Friedman PA (2009) NHERF1 regulates parathyroid hormone receptor desensitization: Interference with beta-arrestin binding. *Mol Pharmacol* 75(5):1189–1197.
10. Bounoutas GS, Tawfeek H, Fröhlich LF, Chung UI, Abou-Samra AB (2006) Impact of impaired receptor internalization on calcium homeostasis in knock-in mice expressing a phosphorylation-deficient parathyroid hormone (PTH)/PTH-related peptide receptor. *Endocrinology* 147(10):4674–4679.
11. Okazaki M, et al. (2008) Prolonged signaling at the parathyroid hormone receptor by peptide ligands targeted to a specific receptor conformation. *Proc Natl Acad Sci USA* 105(43):16525–16530.
12. Feinstein TN, et al. (2011) Retromer terminates the generation of cAMP by internalized PTH receptors. *Nat Chem Biol* 7(5):278–284.
13. Dean T, et al. (2006) Mechanisms of ligand binding to the PTH/PTHrP receptor: Selectivity of a modified PTH(1-15) radioligand for G{Alpha}S-coupled receptor conformations. *Mol Endocrinol* 20:931–942.
14. Dean T, Vilardaga JP, Potts JT, Jr., Gardella TJ (2008) Altered selectivity of parathyroid hormone (PTH) and PTH-related protein (PTHrP) for distinct conformations of the PTH/PTHrP receptor. *Mol Endocrinol* 22(1):156–166.
15. Rey A, Manen D, Rizzoli R, Caverzasio J, Ferrari SL (2006) Proline-rich motifs in the parathyroid hormone (PTH)/PTH-related protein receptor C terminus mediate scaffolding of c-Src with beta-arrestin2 for ERK1/2 activation. *J Biol Chem* 281(50): 38181–38188.
16. Biber J, Hernando N, Forster I, Murer H (2009) Regulation of phosphate transport in proximal tubules. *Pflugers Arch* 458(1):39–52.
17. Qi Z, et al. (2004) Serial determination of glomerular filtration rate in conscious mice using FITC-inulin clearance. *Am J Physiol Renal Physiol* 286(3):F590–F596.
18. Clemens TL, et al. (2001) Parathyroid hormone-related protein and its receptors: Nuclear functions and roles in the renal and cardiovascular systems, the placental trophoblasts and the pancreatic islets. *Br J Pharmacol* 134(6):1113–1136.
19. Massfelder T, et al. (1993) Evidence for adenylyl cyclase-dependent receptors for parathyroid hormone (PTH)-related protein in rabbit kidney glomeruli. *Life Sci* 53(11): 875–881.
20. Buys ES, et al. (2009) sGC(alpha)1(beta)1 attenuates cardiac dysfunction and mortality in murine inflammatory shock models. *Am J Physiol Heart Circ Physiol* 297(2): H654–H663.
21. Datta NS, Samra TA, Mahalingam CD, Datta T, Abou-Samra AB (2010) Role of PTH1R internalization in osteoblasts and bone mass using a phosphorylation-deficient knock-in mouse model. *J Endocrinol* 207(3):355–365.
22. Nagai S, et al. (2011) Acute down-regulation of sodium-dependent phosphate transporter NPT2a involves predominantly the cAMP/PKA pathway as revealed by signaling-selective parathyroid hormone analogs. *J Biol Chem* 286(2):1618–1626.
23. Ba J, Brown D, Friedman PA (2003) Calcium-sensing receptor regulation of PTH-inhibitable proximal tubule phosphate transport. *Am J Physiol Renal Physiol* 285(6): F1233–F1243.
24. Goldsmith RS, Ingbar SH (1966) Inorganic phosphate treatment of hypercalcemia of diverse etiologies. *N Engl J Med* 274(1):1–7.
25. Neufeld A, Collip J (1942) The primary action of the parathyroid hormone. *Endocrinology* 30:135–141.
26. Albright F, Bauer W, Claflin D, Cockrill JR (1932) Studies in parathyroid physiology: III. The effect of phosphate ingestion in clinical hyperparathyroidism. *J Clin Invest* 11(2): 411–435.
27. Felsenfeld AJ, Rodriguez M (1999) Phosphorus, regulation of plasma calcium, and secondary hyperparathyroidism: A hypothesis to integrate a historical and modern perspective. *J Am Soc Nephrol* 10(4):878–890.
28. Parsons JA, Neer RM, Potts JT, Jr. (1971) Initial fall of plasma calcium after intravenous injection of parathyroid hormone. *Endocrinology* 89(3):735–740.
29. Parsons JA, Robinson CJ (1971) Calcium shift into bone causing transient hypocalcaemia after injection of parathyroid hormone. *Nature* 230(5296):581–582.
30. Raisz LG, Niemann I (1969) Effect of phosphate, calcium and magnesium on bone resorption and hormonal responses in tissue culture. *Endocrinology* 85(3):446–452.
31. Okazaki M, Potts JJ, Gardella T (2008) Identification and optimization of residues in PTH and PTHrP that determine altered modes of binding to the PTH/PTHrP receptor. *J Bone Min Res* 23(S1):Sa224, Abstract.
32. Binkowski BF, et al. (2011) A luminescent biosensor with increased dynamic range for intracellular cAMP. *ACS Chem Biol* 6(11):1193–1197.
33. Wittelsberger A, Thomas BE, Mierke DF, Rosenblatt M (2006) Methionine acts as a "magnet" in photoaffinity crosslinking experiments. *FEBS Lett* 580(7):1872–1876.